Journal of the Korean Chemical Society
2009, *Vol. 53, No. 3*
Printed in the Republic of Korea

$La_7Os_4C_9$의 전자구조와 화학결합

강 대 복*
경성대학교 화학과
(2009. 5. 1 접수)

Electronic Structure and Chemical Bonding of $La_7Os_4C_9$

Dae-Bok Kang*
Department of Chemistry, Kyungsung University, Busan 608-736, Korea
(Received May 1, 2009)

요 약. 고체 화합물 $La_7Os_4C_9$ 속에 있는 $[Os_4C_9]^{21-}$ 사슬의 전자구조와 화학결합을 extended Hückel 계산 결과에 의해서 논의하였다. 탄소 원자는 물론 $(C_2)^{2-}$ 분자의 결합 특성은 비교적 큰 Os-C 상호작용을 나타내었고 특히 $(C_2)^{2-}$ 분자의 결합길이 증가는 Fermi level 바로 아래에 Os-$C_2(1\pi_g)$ 결합 밴드의 존재로 인해서 반결합 $1\pi_g$ 오비탈에 부분적인 전자점유가 일어나기 때문인 것으로 해석된다.

주제어: Ternary transition metal carbide, Electronic structure, Extended Hückel calculations, FMO analysis

ABSTRACT. In the recently synthesized rare earth transition metal carbide $La_7Os_4C_9$ one finds one-dimensional organometallic $[Os_4C_9]^{21-}$ polymers embedded in a La^{3+} ionic matrix. The electronic structure of the polymeric $[Os_4C_9]^{21-}$ chain was investigated by density of states (DOS) and crystal orbital overlap population (COOP), using the extended Hückel algorithm. A fragment molecular orbital analysis is used to study the bonding characteristics of the C_2 units in $La_7Os_4C_9$ containing C_2 units and single C atoms as well. The title compound contains partially filled Os and carbon bands leading to metallic conductivity. As the observed distances already indicated, the calculations show extensive Os-C interactions. The C-C bond distance in the diatomic C_2 units (d_{C-C}=131 pm) in the solid is significantly increased relative to C_2^{2-} or acetylene, because antibonding $1\pi_g$ orbitals are partially filled by the Os-$C_2(1\pi_g)$ bonding contribution found at and below the Fermi level.

Keywords: Ternary transition metal carbide, Electronic structure, Extended Hückel calculations, FMO analysis

INTRODUCTION

A large number of ternary carbides of the rare earth elements with transition metals have been synthesized in the recent years.[1-7] The rare earth element in these ternary systems is a highly electropositive multivalent metal. Complete ionization of the electropositive metal leads to a transition metal-carbon polyanionic substructure where the carbon atoms are more or less covalently bonded to the transition metal atoms, frequently forming organometallic polymers. These compounds exhibit structural diversity, containing isolated carbon atoms, C_2 pairs and C_3 units. One also finds in them interesting metal-carbon networks of varying dimensionality.

In this paper, we turn our attention to a new one-dimensional organometallic polymer in the ternary compound $La_7Os_4C_9$ with mixed carbon ligand types, synthesized by Wagner and Kniep.[1] Two types of C_n (n=1, 2) units are present in the structure, yielding the unit cell composition

La-$Os_4(C_2)_2C_5$. The Os-C sheets have two types of carbon atoms, each bridging two Os atoms in either a linear or a bent geometry and the C_2 pairs occupying terminal positions.

The electronic structure of this compound is studied with the results of extended Hückel tight-binding (EHTB) calculations.[8] The exponent (ζ) and the valence shell ionization potential (H_{ii} in eV) were respectively used in the molecular and tight-binding calculations as follows: 1.625, -21.4 for C 2s; 1.625, -11.4 for C 2p; 2.452, -8.17 for Os 6s; 2.429, -4.81 for Os 6p; 2.14, -7.67 for La 6s; 2.08, -5.01 for La 6p. H_{ii} values for Os 5d and La 5d were set equal to -11.84 and -8.21 eV, respectively. A linear combination of two Slater-type orbitals of exponents ζ_1 = 5.571, ζ_2 = 2.416 and ζ_1 = 3.78, ζ_2 = 1.381 with weighting coefficients c_1 = 0.6372, c_2 = 0.5598 and c_1 = 0.7765, c_2 = 0.4586 was used to represent the 5d atomic orbitals of Os and La, respectively. The crystal structure of La-Os_4C_9 was used for the calculations. The selected bond lengths and angles listed in *Table* 1. Sets of 396 k points chosen in the corresponding irreducible Brillouin zone were utilized for the calculations of the density of states, crystal orbital overlap populations, and atomic net charges. A fragment molecular orbital (FMO) analysis is used to gain information about the bonding interactions of the C_2 units. In electronic structure calculations the interactions between atoms can be examined by density of states (DOS) and crystal orbital overlap population (COOP). The COOP can be looked upon as the DOS weighted by the overlap integral S_{ij} between two chemical species i and j. In the plots, positive and negative magnitudes of COOP are indicative of bonding and antibonding interactions, respectively.

Table 1. Selected bond lengths (pm) and angles (deg) for $La_2Os_4C_9$

Os1-C2	194.3	Os1-C1	196.7
Os1-C1	207.4	Os2-C5	192.3
Os2-C3	192.9	Os2-C2	193.0
Os1-Os1	271.6	C3-C4	131.6
Os1-C1-Os1	84.4	C1-Os1-C1	95.6
C1-Os1-C2	150.9	C1-Os1-C2	113.5
Os1-C2-Os2	172.9	C2-Os2-C3	119.4
C2-Os2-C5	114.8	Os2-C3-C4	162.9

RESULTS AND DISCUSSION

Crystal structure

The title compound crystallizes in the monoclinic space group C2/m with two formula units per cell.[1] The crystal structure of La-Os_4C_9 is shown in *Figure* 1. Quasi-one-dimensional polymers of stoichiometric Os_4C_9 are well separated in the lattice. The polymeric structure comprises covalent chains of $[Os_4(C_2)_2C_5]^{2-}$ extended along the crystallographic *c* axis with La^{3+} ions in between. All the atoms along the chain are in the same plane. Two types of carbon species, bridging C atoms and terminal C_2 pairs are clearly distinguishable. Both are situated in distorted metal octahedra.

The polymeric anions are composed of alternating $Os(C_2)C_2$ and OsC_3 units with osmium atoms in distorted trigonal planar coordination (*Figure* 1). Os1 has three C neighbors at distances covering the range from 194 to 207 pm. Two of them form Os_2C_4 fragments with an Os–Os distance of 272 pm (270 pm in elemental Os) via the common

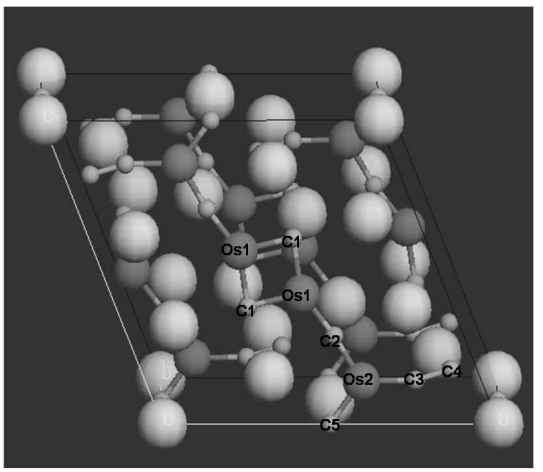

Fig. 1. Unit cell of the monoclinic $La_2Os_4C_9$ structure. The lanthanum, osmium, and carbon atoms are drawn as large, medium, and small circles, respectively. The one-dimensional $[Os_4C_9]^{2-}$ polyanionic chains are emphasized.

C···C edge. The Os2 atoms are surrounded by two C atoms and one end-on C_2 pair at the rather short distance of about 193 pm. The sum of the covalent radii of osmium and carbon is 203 pm.[9] Hence the average Os-C bond distance of 196 pm is somewhat shorter than that expected for a single bond. We thus ascribe some double bond character to the Os-C bonding interactions. The angles C–Os1–C within the OsC_3 unit range between 95.61° and 150.81° and the angles C–Os2–C in the $Os(C_2)C_2$ unit between 114.91° and 125.81°. The C_2 pairs display a C–C bond distance of 131 pm. This value is slightly larger than the carbon–carbon triple bond length in acetylene (121 pm), suggesting an intermediate bonding situation between a C-C triple bond and a double bond (134 pm). This ligand may be considered to be the dinegative $(C_2)^{2-}$ derived from the deprotonation of a vinylidene ligand $H_2C=C=M$.

The La atoms are surrounded in a distorted square planar, tetrahedral and trigonal bipyramidal way by carbon atoms at separations ranging from 263 to 282 pm. These distances are all slightly longer than the metallic radius of lanthanum (169 pm) and the single-bond radius of carbon (77 pm) which add up to 246 pm. The La atoms have La neighbors at distances between 348 and 390 pm, while the Os atoms have La neighbors at distances between 314 and 332 pm. These distances are very similar to the sum of the metallic radii of 374 pm for La-La and 322 pm for La-Os. Although the La-C and La-Os interactions at these distances are not negligible, the Os-C interactions are certainly most significant. All interatomic distances are comparable to those found in the crystal structure of $La_5Os_3C_{4-x}$.[7]

Calculations on the entire three-dimensional Os_4C_9 sublattice in $La_7Os_4C_9$ and on the whole crystal lattice of $La_7Os_4C_9$ result in similar DOS curves. The COOP calculations on the latter indicate that the La-C (OP=0.18) and La-Os (OP=0.09) interactions are much weaker than the Os-C (OP = 0.67) ones. The fact that covalent bonding of Os-C bonds is stronger compared with La-C ones forms the basis for separating the complex carbometalate anion from the La substructure. Furthermore, even though La-C interactions reveal a significant covalent character, the oxidation states of the La atoms have to be considered as +3 since no La majority band states are occupied below the Fermi level. This gives us confidence that the formula of this compound can, to a first approximation, be written as $La^{3+}[Os_4C_9]^{21-}$, emphasizing the covalent Os-C bonding in the polyanionic units.

Electronic structure of polymeric $[Os4C9]^{21-}$ chains

As outlined above, the chemical bonding in the $La_7Os_4C_9$ carbide can be rationalized by simple electron counting, assuming complete charge transfer of all valence electrons of the lanthanum atoms to the $[Os_4C_9]$ moieties. We first consider a molecular model, $[OsC_3]^{11-}$, in a trigonal planar coordination geometry with D_{3h} symmetry. *Figure* 2 shows schematically how the orbitals on Os atoms interact with those on carbon ligands. Since carbon 2s orbitals are very low in energy, and Os 6p orbitals are high up in energy, both contribute little to Os-C bonding. Our parameters place the Os 5d orbitals just below the carbon 2p orbitals and the Os 6s orbital above the carbon 2p orbitals. The major bonding interactions occur between carbon 2p orbitals and Os 5d orbitals. At the bottom of the diagram we find five Os 5d orbitals to form five Os-C bonding orbitals with symmetry-adapted com-

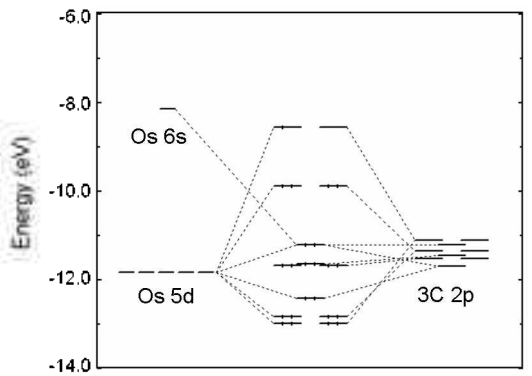

Fig. 2. MO diagram for the model compound $[OsC_3]^{11-}$ in a trigonal planar geometry with D_{3h} symmetry. All Os-C bond lengths are set to 196 pm.

binations from the carbon ligands. There should be five Os-C antibonding orbitals at the top of the diagram. We only see four of them. The missing one should involve the Os $5dz^2$ orbital; however, mixing in of the Os 6s orbital in a bonding way turns this Os-C antibonding combination into an essentially Os-C nonbonding orbital, located just above the five Os-C bonding orbitals. In the middle of the energy diagram, four carbon-based nonbonding orbitals are located.

It is useful to have some knowledge of the electronic structure of an isolated C_2 entity, which plays a crucial role in the solid. A C_2 molecule with a bond length of 131 pm has the molecular orbitals of a typical homonuclear diatomic. Mixing of the 2s and one 2p atomic orbitals (AOs) leads to four σ-type molecular orbitals (MOs): one strongly bonding ($2\sigma_g$), two nonbonding combinations ($2\sigma_u$ and $3\sigma_g$), and one strongly antibonding ($3\sigma_u$), very high in energy. The other 2p orbitals form pairs of degenerate bonding $1\pi_u$ and antibonding $1\pi_g$ MOs. The energy levels of these orbitals are shown in *Figure* 3. The large gap computed between the nonbonding $3\sigma_g$ and antibonding $1\pi_g$ MOs (3.02 eV) would lead us to assign a count of 10 electrons for the isolated C_2 pairs. Note that the triple-bond character is retained for the formal charge of 2- per C_2.

Figure 3 displays the C_n (n=1, 2) DOS contributions to the total carbon sublattice of the $La_7Os_4C_9$ structure. In the case of the isolated C atom two

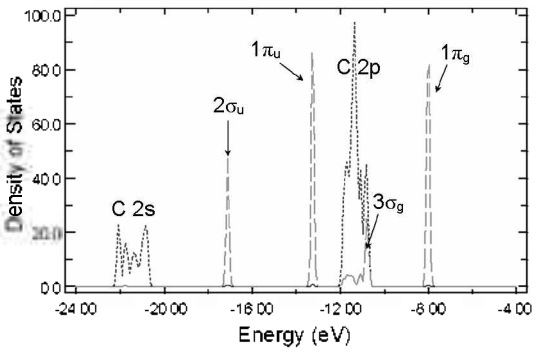

Fig. 3. DOS contributions of different carbon species C (dotted line, red) and C_2 (dashed line, green) to the total carbon sublattice in the $La_7Os_4C_9$ structure.

block bands corresponding to the 2s and 2p levels of C are clearly seen centered around the relevant orbital energies of -21.4 and -11.4 eV as expected. For C^{4-} all levels would be filled; the Fermi level is located at *ca.* -10.6 eV. The DOS contributions of the C_2 units to the total carbon DOS are consistent with the MO levels described above. The ordering of levels for C_2, in the window shown in *Figure* 3, is $2\sigma_u$, $1\pi_u$, $3\sigma_g$ and $1\pi_g$ with increasing energy. For a formal charge of $(C_2)^{2-}$ the $3\sigma_g$ band would be completely filled, with the Fermi level located at *ca.* -10.6 eV. If the electron occupations were $(C_2)^{4-}$, the antibonding $1\pi_g$ states would be partially filled. Therefore, on the basis of the orbital occupations of C and C_2 units, the charge distribution $(La^{3+})_7(Os^{0.75-})_4(C_2^{2-})_2(C^{4-})_5$ constitutes a good oxidation state formalism to start with.

Covalent interactions between the Os atoms and the anionic entities must transfer somewhat of the anionic charge of the latter. The DOS plot for $[Os_4C_9]^{21-}$ is shown in *Figure* 4, along with the contribution of Os, bridging carbon atoms, and terminal C_2 pairs to the total DOS. The interactions between carbon and osmium result in strong orbital mixing, and thus the Os contribution is spread out over the whole energy range, indicating extensive Os-C bonding interactions. A decomposition of the contribution to the DOS of the different elements

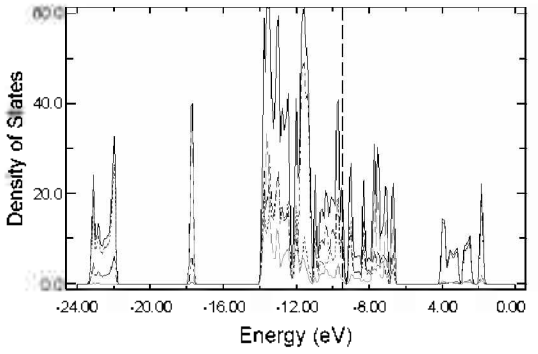

Fig. 4. Total DOS of the composite $[Os_4C_9]^{21-}$ structure assembled from the sublattices of carbon and Os. C, C_2, and Os contributions to the total DOS (solid line, black) are marked by dotted (red), dashed (green), and dash-dot lines (blue), respectively. The dashed line at *ca.* -9.49 eV refers to the Fermi level.

indicates that the lowest part, centered at -22.5 eV, derives mainly from the bridging carbon atoms. The projection on the C atoms indicates that most of the valence states of this atom are occupied, in agreement with its C^{4-} oxidation state. The C_2 $2\sigma_u$ and $1\pi_u$ bands, centered at -17.8 and around -13.5 eV, respectively, are pushed down in energy by the interaction with the Os d bands. The $3\sigma_g$ and $1\pi_g$ orbitals, on the other hand, interact strongly with the Os d bands, spreading out over their energy range -12 to -6.5 eV. The $3\sigma_g$ orbitals (-12 to -11 eV) are lowered, relative to the corresponding levels of the isolated C_2. The important participation of $1\pi_g$ orbitals is noticed at and just below the Fermi level (-11 to -9 eV), although one finds states predominantly metallic in character. This portion is the Os-C_2 bonding (weakly C-C antibonding) combination, with the Os-C_2 antibonding combination (C-C antibonding) at higher energy, ranging from -8 to -6.5 eV, which is composed mainly of $1\pi_g$ orbitals. This is confirmed by the C_2 COOP curve represented in *Figure* 5, which shows that C_2 antibonding $1\pi_g$ states are partially occupied near the Fermi level after interaction with the metallic host. Partial electron occupation of the low-lying Os-C_2($1\pi_g$) bonding states introduces a weakening to the C-C bond. Consistent with this occupation, the C-C bond length expands from the expected value for a C-C triple bond of about 121 pm to 131 pm. The $1\pi_g$ levels of the C_2 unit are occupied in $[Os_4C_9]^{21-}$ by approximately 0.79 electrons, as obtained from an FMO analysis (see *Table* 2). For a triple bond in $(C_2)^{2-}$ the MO levels are filled with 10 electrons up through the $3\sigma_g$ level. Introducing two more electrons would lead to a partial occupation of antibonding $1\pi_g$ levels and thus a C-C double bond. The $1\pi_g$ occupation of 0.79 in $[Os_4C_9]^{21-}$ leads to a C-C bonding situation best described as an effective bond order between a double and a triple bond. The C-C overlap population, which is 1.74, calculated for the isolated $(C_2)^{2-}$ entity, drops to 1.55 after interaction with the metallic host.

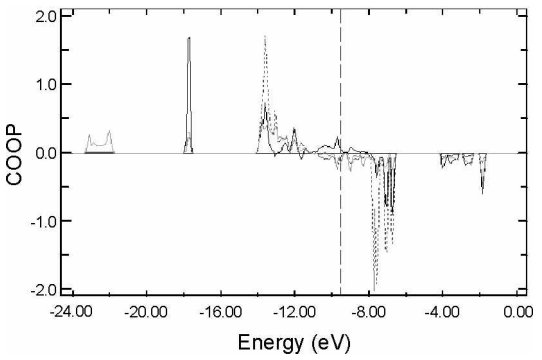

Fig. 5. COOP curves for Os-C_2 (solid line, black), C-C (dotted line, red), and Os-C (dashed line, green) bonds in $[Os_4C_9]^{21-}$ structure. The dashed line at *ca.* -9.49 eV refers to the Fermi level.

The calculated net atomic charges and FMO occupations are given in *Table* 2. The Mulliken population analysis gives net atomic charges of $Os^{-1.69}$, bridging $C^{-1.99}$, and terminal $C_2^{-2.16}$, substantially different from their formal oxidation states. The atomic net charges reported in *Table* 2 reflect electron transfer from the C^{4-} toward the Os and from the Os toward the C_2 units. These strong covalent interactions between the different elements in the solid manifest themselves also through the highly positive Os-C overlap population, which is 0.78 (*Table* 2). The COOP curves, given in *Figure* 5, indicate that the Os-C bonding is not maximized with some Os-C antibonding states occupied. The Os-C COOP curve shows clearly the transition from the Os-C bonding to antibonding region at

Table 2. Bonding characteristics computed for the $[Os_4C_9]^{21-}$ structure

	$[Os_4C_9]^{21-}$	$(C_2)^{2-}$
Overlap populations:		
Os-C	0.78	
Os-C_2	0.86	
C-C	1.55	1.74
Os-Os	0.07	
Atomic net charges:		
Os	-1.69	
C_2	-2.16	-2.00
C	-1.99	
FMO occupations:		
$2\sigma_g$	1.97	2
$2\sigma_u$	1.82	2
$1\pi_u$	3.94	4
$3\sigma_g$	1.64	2
$1\pi_g$	0.79	0

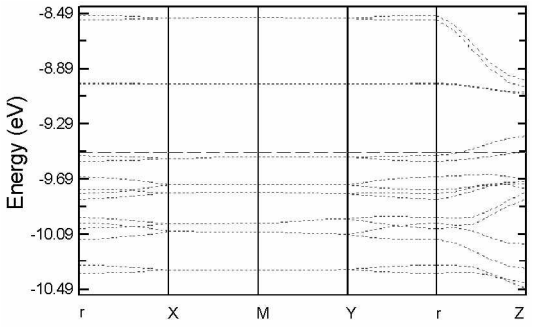

Fig. 6. Band structure of $[Os_4C_9]^{21-}$ sublattice. The dashed line at *ca.* -9.49 eV refers to the Fermi level.

-11 eV. The Fermi level comes at slightly higher energy (-9.49 eV), in a region of substantial Os-C antibonding. A generalization that seems to hold is that structures maximize bonding. Given that the bands at the Fermi level are Os-C antibonding for $La_7Os_4C_9$, more stable structures should be formed on removing some electrons from the system. The Os and C contributions at the Fermi level are primarily due to the participation of the Os and bridging C and to a lesser extent of the antibonding $1\pi_g$ MOs. The position of the Fermi level cutting a rather narrow and sharp peak in the DOS indicates that $La_7Os_4C_9$ should be metallic.

A section of the band structure of $[Os_4C_9]^{21-}$ sublattice is shown in *Figure* 6. The bands remain dispersionless in various directions of the reciprocal space. The Fermi level, at *ca.* -9.49 eV, crosses more dispersive bands along the crystallographic *c* axis, allowing electrical conductivity along the $[Os_4C_9]^{21-}$ chain direction. Electrical resistivity measurements revealed a temperature dependence typical for a metal,[1] in agreement with our electronic structure calculations.

CONCLUDING REMARKS

The electronic structure of $[Os_4C_9]^{21-}$ presents us with highly covalent interactions of the transition metal with the unperturbed energy levels of the C atom and C_2 units. Oxidation state formalism of $(La^{3+})_7(Os^{0.75+})_4(C_2^{2-})_2(C^{4-})_5$ for $La_7Os_4C_9$ constitutes a good starting point to describe its electronic structure. The formal charge of C^{4-} is consistent with our calculations. Of course, this charge is reduced by covalent interactions with Os. For the C_2 unit, we find antibonding $1\pi_g$ states occupied near the Fermi level, displaying a reduced triple-bond character, and thereby causing the increase of the C-C bond length. The bonding of the C_2 units is characterized by strong Os-$C_2(3\sigma_g)$ and Os-$C_2(1\pi_g)$ interactions. The Fermi level cuts a narrow and sharp peak in the DOS composed mainly of Os-C antibonding states and to a lesser extent of Os-$1\pi_g$ bonding states. This allows us to conclude that the rather important occupation of the antibonding $1\pi_g$ MOs and the depopulation of the bonding MOs, particularly the $3\sigma_g$ one are responsible for the significantly weakened C-C triple bond strength after interaction. According to the band structure, dispersive bands are observed along the polymeric $[Os_4C_9]^{21-}$ chain direction. This compound should be a 1D-like metal.

Acknowledgments. This work was supported by the Kyungsung University Research Grant in 2009.

REFERENCES

1. Dashjav, E.; Prots, Y.; Kreiner G.; Schnelle, W.; Wagner, F. R.; Kniep, R. *J. Solid State Chem.* **2008**, *181*, 3121.
2. Dashjav, E.; Kreiner, G.; Schnelle, W.; Wagner, F. R.; Jeitschko, W.; Kniep, R. *J. Solid State Chem.* **2007**, *180*, 636.
3. Kahnert, G. E.; Jeitschko, W.; Block, G. *Z. Anorg. Allg. Chem.* **1993**, *619*, 442.
4. Hoffmann, R.-D.; Pottgen, R.; Jeitschko, W. *J. Solid State Chem.* **1992**, *99*, 134.
5. Pottgen, R.; Jeitschko, W. *Z. Naturforsch. b*, **1992**, *47*, 358.
6. Gerdes, M. H.; Jeitschko, W.; Wachtmann, K. H.; Danebrock, M. E. *J. Mater. Chem.* **1997**, *7*, 2427.
7. Wachtmann, K. H.; Hufken, T.; Jeitschko, W. *J. Solid State Chem.* **1997**, *131*, 49.
8. (a) Hoffmann, R. *J. Chem. Phys.* **1963**, *39*, 1397. (b) Whangbo, M.-H.; Hoffmann, R. *J. Am. Chem. Soc.* **1978**, *100*, 6093.
9. Pauling, L. *The Nature of the Chemical Bond*; Cornell University Press: New York, 1960.